Sail aerodynamics: on-water pressure measurements on a downwind sail

Sail Aerodynamics: On-Water Pressure Measurements on a Downwind Sail

Ignazio Maria Viola* and **Richard G. J. Flay**[†]

*Yacht and Superyacht Research Group, School of Marine Science and Technology, Newcastle University, United Kingdom
[†]Yacht Research Unit, The University of Auckland, New Zealand

Pressures on three horizontal sections of a downwind sail were measured for several wind directions and sail trims. The pressure distributions were compared with wind tunnel tests; similarities and differences were found, the latter as a result of the dynamic effects, which were not modeled in the wind tunnel. A pressure distribution at the head of the spinnaker resembling that from a delta wing was measured at an apparent wind angle of 120°.

Keywords: sail aerodynamics; downwind sail; asymmetric spinnaker; pressure measurements; full-scale tests; model-scale tests; wind tunnel tests

1. Introduction

Sail aerodynamics have been widely investigated in the last century. Sails made from different materials and made in different shapes have been compared with full-scale tests, wind tunnel tests, and numerical computations. These three approaches allow different aspects of sail aerodynamics to be investigated. Unfortunately, each of them has some limitations, and none of them is able to substitute for the other two. The present article investigates sail aerodynamics in downwind sailing conditions from on-water tests.

1.1. Computational fluid dynamics

In the past few decades, numerical programs have become the most commonly used research tool for sails. In the 1960s, potential-flow computational methods were used for two-dimensional horizontal sail sections. In the following years, the fast growth of computational resources led to Navier-Stokes solvers being used more and more frequently. Sails behave very differently in upwind and downwind conditions. A yacht sails upwind or downwind when the supplementary angle (called the true wind angle) between the wind velocity and the yacht velocity is lower or higher than 90°, respectively. Nowadays, although potential-flow solvers are widely used for upwind sailing conditions, Navier-Stokes programs are most commonly used for downwind conditions. In fact, in upwind sailing conditions, the sails are expected to often operate near the maximum lift/drag ratio where the flow would have an attached boundary layer on most of the sail surface. Potential-flow codes, which are unable to model separated boundary layers, can compute aerodynamic forces with a reasonable accuracy in upwind conditions. Conversely, in downwind sailing conditions, sails are designed to operate nearer the maximum lift and, therefore, they have more cambered sections and higher pressure gradients. The boundary layer separates before the trailing edge over a large part of the sail surface as a result of the high adverse pressure gradients. To correctly compute the aerodynamic forces, separation has to be computed correctly by modeling the effects of viscosity of the fluid. Therefore, Navier-Stokes computational fluid dynamic programs are most commonly used to model downwind sail aerodynamics.

As a result of the relatively high sail Reynolds number, at the present time, direct Navier-Stokes computations cannot be used in sail aerodynamics, even when very large computational resources are available (Viola & Ponzini 2011). Therefore, Reynolds Averaged Navier-Stokes (RANS), Large Eddy Simulations (LES), or Detached Eddy Simulations (DES) techniques have to be used to model the small-scale turbulence neglected by the limited grid resolution. These techniques use based on heuristic equations, which need to be validated with experimental measurements. Validations should be repeated every time the modeled geometry or the fluid characteristics are changed significantly. Wind tunnel tests can be performed for this purpose.

Manuscript received at SNAME headquarters October 26, 2011; revised manuscript received November 28, 2011.

1.2. Wind tunnel tests

Wind tunnel tests allow the designer to have a real-time aerial view of the flying sails. Smoke visualization or other similar techniques allow streaklines to be visualized very efficiently. At the Yacht Research Unit of the University of Auckland, forces are measured with a six-component balance located below the wind tunnel floor. It is common practice to use flexible sails, which can be trimmed remotely. Therefore, the change of forces and streaklines with change in the sail trim can be appreciated immediately. In most of the wind tunnels in which sail aerodynamics is investigated, special devices allow the flying shapes to be detected. Thus, the aerodynamic forces and flying shapes are recorded simultaneously. This increases the repeatability of the measurements and allows differences between sails and trims to be better appreciated. It also allows flying shapes to be modeled with numerical solvers and computed forces to be compared with measured forces. However, validating numerical simulations just with forces is not ideal. In fact, the pressure distribution on sails might well be computed incorrectly even when the computed resultant aerodynamic forces agree with the measured forces. This is because different pressure distributions can lead to the same global aerodynamic force. For this reason, in recent years, a great deal of effort has been put into measuring pressure distributions on sails with the aim of validating numerical programs (Viola et al. 2011).

Using flexible sails in wind tunnel tests allows different trims to be investigated. The deformation of the mast should be correctly modeled because it has a significant effect on the sail shape and on the sail position with respect to the longitudinal boat axis. Wind tunnel tests are usually performed at wind speeds between 2 m/s and 5 m/s. In wind tunnels with the large test sections, the model scale is of the order of 1/10 of full scale. As a consequence, to achieve the full-scale Reynolds number, the wind tunnel wind speed should be 10 times higher than the full-scale wind speed. Unfortunately, however, the maximum wind tunnel wind speed is usually equal to or less than the full-scale wind speed. This is because the flexible sails and rigging do not allow testing in high-speed conditions, because they would break!

The attitude of a sail flying high and far from the yacht depends on the ratio between the aerodynamic force developed by the pressure distribution and the gravity force. Therefore, the weight of the model-scale sails should be chosen to achieve the same full-scale ratio between the pressure forces and the gravity force. This criterion leads to the choice of a very light model-scale sailcloth. However, because the sail is a membrane, such a lightweight cloth would stretch a considerable amount as a result of the loads it would be subjected to, and this change in shape would alter the aerodynamic loading. Unless the mast is especially bendy, where it needs to bend in the wind tunnel tests, the mast is usually modeled in its deformed "sailing" shape and, often, the sail is cut to its "flying" shape. Thus, the sails are tested in the wind tunnel at the correct flying attitude and thus properly simulate full scale.

1.3. On-water tests

Both numerical simulations and wind tunnel tests are simplified models of the complex full-scale conditions. When yachts sail, the dynamic movements of the yacht and of the sails are considerable. Moreover, the yacht sails through the turbulent atmospheric boundary layer, which leads to a time-dependent flow pattern. The sails are continuously trimmed to take into account the dynamic movements of the yacht, the sails, and the change in the wind speed and direction. All these dynamic effects are modeled with difficulty (and consequently with low accuracy) in computational fluid dynamics (CFD) and are normally not modeled in wind tunnels, except in special "dynamic" tests.

Because of the complexity of these dynamic effects, on-water tests are very difficult to perform and suffer from poor repeatability, thus leading to a large uncertainty in the results. First, the fully three-dimensional time-dependent wind flow, in which the yacht sails, cannot be measured. For instance, if an anemometer were fixed on the top of the mast to measure the three wind velocity components, the measurement would be affected significantly by the influence of the sail trim. Moreover, even if the flow field was known at a location near the top of the mast, the apparent wind speed and direction change significantly between the top of the mast and sea level as a result of the apparent wind vector being formed by subtracting the yacht velocity off the true wind velocity, and their differences vary considerably between the foot and head of a sail.

Both forces and pressures can be measured onboard. As mentioned previously, measuring the pressure distributions is preferable to measuring forces, because it gives a much more complete description of the loading process. It is more difficult to make pressure measurements in downwind conditions than in upwind sailing conditions because the apparent wind speed and thus the pressure differences measured by the transducer are lower in the former case. The apparent wind velocity is the vectorial difference between the true wind velocity and the velocity of the yacht. The apparent wind angle (AWA) is the supplementary angle between the apparent wind velocity and the velocity of the yacht, whereas the apparent wind speed (AWS) is the modulus of the apparent wind velocity.

The differential pressure across sails is of the order of magnitude of the dynamic pressure, which is, for instance, approximately 5.5 Pa for a 3 m/s AWS. To measure a pressure distribution along a sail section, pressure variations smaller than approximately 1 Pa should be measured. However, 1-Pa pressure change corresponds to a wind speed change as small as 0.3 m/s. Moreover, pressures can change by several pascals per minute as a result of the incoming atmospheric turbulence. The lower AWS means that these pressure changes from turbulence are superimposed on lower mean values, giving the effect of increased unsteadiness.

Therefore, on-water pressure measurements automatically take into account these dynamic effects, which are neglected or poorly modeled by numerical simulations and wind tunnel experiments, but on the other hand, the complexity of the real sailing situation makes the measurements quite complicated to perform and difficult to interpret because the boundary conditions (i.e., the onset flow conditions) are not known precisely and so considerable judgment has to be used to decide on the appropriate boundary conditions to be prescribed in any CFD or wind tunnel comparisons.

1.3.1. The state of the art of pressure measurements on sails. Sail aerodynamics have been widely investigated with numerical modeling. From the 1960s to the end of the last century, most of the computations were performed using potential flow codes. In the past 10 years, RANS codes have become very popular for studying downwind sails. A review of potential flow and RANS applications is presented in Viola (2009). Over the past few years, only a few LES or DES applications on sails have been published (Braun & Imas 2008; Wright et al. 2010), but the most important research institutes in sail aerodynamics are all investigating these techniques.

Viola and Flay (2009) review wind tunnel force measurements on downwind sails, whereas Viola and Flay (2010a) review pressure measurements on sails performed on the water and in a wind tunnel. In the following paragraphs, a complementary review of force and pressure full-scale experiments on sails is provided.

Force measurements have been performed more rarely in full scale than in wind tunnels as a result of the associated difficulty and cost. Milgram et al. (1993), at the Massachusetts Institute of Technology (MIT), introduced the innovative concept of an instrumented framework structure located inside the 35-ft. yacht Amphetrete. The frame connected the rigging to the hull and was instrumented with a six-component balance that measured the aerodynamic forces in equilibrium with the hydrodynamic forces. Masuyama and Fukasawa (1997), at the Kanazawa Institute of Technology, developed a similar concept on the yacht Fujin. These two articles are mainly oriented toward investigating the aerodynamics of yachts. Conversely, the research described by Hochkirch and Brandt (1999) at the Berlin University was mainly focused on the hydrodynamics of yachts. They applied a similar "space-frame structure" concept to the 33-ft. yacht Dyna as well as having an additional anemometer and were able to measure the hydrodynamic forces on the yacht appendages.

Full-scale pressure measurements were performed for the first time by Warner and Ober (1925) at the MIT (the tests were performed between 1915 and 1921). The authors used U-tube pressure manometers on the S-class yacht Papoose. Much later, Flay and Millar (2006) reported the lessons learned by the Yacht Research Unit (YRU) of the University of Auckland in measuring pressures on the sails of the Farr1020-class yacht Shokran. The first pressure distribution with a large number of pressure taps (25 per side) was presented the same year by Puddu et al. (2006) from the University of Cagliari, Sardinia. The authors measured the pressures on the mainsail of a Tornado-class catamaran. Gaves et al. (2008) measured the pressures on the mainsail of a IACC-class yacht, but only five pressure taps were used. The first modern pressure measurements (Warner & Ober 1925) on headsails was recently performed by Viola and Flay (2010b). The authors measured pressure distributions on the mainsail and the genoa of the 24-ft. yacht Aurelie designed by Sparkman & Stephens.

As far as is known by the authors, full-scale pressure distribution on downwind sails has never been published. The present article presents the first pressure measurements on an asymmetric spinnaker. The measurements were performed on a third-scale sail, which was designed for a 90-ft. America's Cup class (AC33) yacht. The sail was tested on a 25-ft. Platu25-class yacht.

2. Method

2.1. The sails

The America's Cup is the oldest trophy and richest prize in sport. It has been sailed at irregular intervals every few years since 1852. In the previous few decades, the challenger who races against the defender of the trophy has been selected by winning the Louis Vuitton Cup in the challenger series. The defender has the privilege of choosing the yacht class rule. In late 2008 and early 2009, it was not clear which yacht class would be used in the 34th America's Cup and when and where the race would be held. Emirates Team New Zealand, the winner of the previous Louis Vuitton Cup, was investigating the design of the most likely class for the next event. The YRU, which was Emirates Team New Zealand's Official Scientific Advisor, asked North Sails New Zealand to manufacture a third-scale AC33-class asymmetric spinnaker for on-water testing. The luff (leading edge), leach (trailing edge), and feet of the sail were 9.2 m, 8 m, and 4.9 m, respectively.

The spinnaker was built with four horizontal panels, which were sewn together with an overlap of approximately 100 mm at each joint. The overlapped panels made three horizontal pockets where 21 pressure taps per pocket were located, and the pockets were used to contain the tubes. The girths of the sail at one-fourth, half, and three-fourths of the height between the head and foot of the sail corresponding to the positions of the bottom, mid-, and top pockets were measured to be 5.5 m, 5 m, and 2.9 m, respectively. On each of them, the measuring holes of the first and last pressure taps were 40 mm from to the luff and the leach respectively. Figure 1 shows a schematic drawing of the pressure taps located along the three overlapping joints.

The pressure taps used were thin plastic frusta with base and top surface diameters of 50 mm and 40 mm, respectively. The frustum height was 5 mm. The pressure taps had a hole in the center of the top surface, which connected to a 2-mm diameter metal tube protruding out the side of the tap, as shown in Fig. 2. Polyvinyl chloride tubes connected to the pressure taps conveyed the pressures to the transducers located inside the yacht cabin. The tubes from all the pressure taps were threaded to the luff (leading edge of the sail) inside the horizontal pockets and then down to the tack (corner of luff and sail foot) inside an additional vertical pocket.

The pressure distributions were measured on the leeward side while sailing on starboard tack (wind coming from the right-hand side of the yacht) and on the windward side when sailing on the port tack (wind coming from the left-hand side of the yacht). No pressure measurements were performed on the mainsail. Future research should aim to measure the pressures on the two sails simultaneously. The mainsail used in the on-water tests was a standard Platu25-class mainsail.

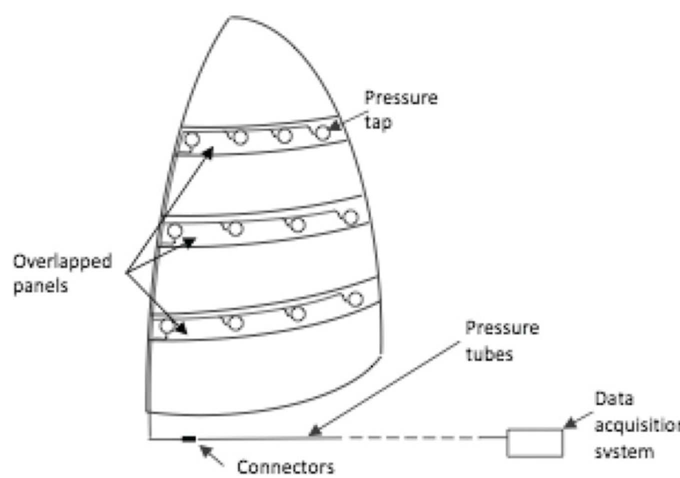

Fig. 1 Schematic layout of the pressure-tapped sail (edited from Watier 2010)

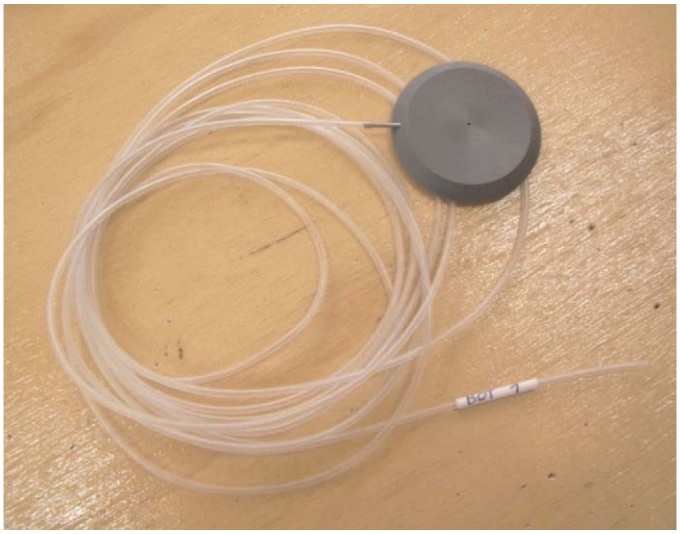

Fig. 2 Pressure tap with pressure tube connected

2.2. The pressure system

The tubes were connected to the transducers, which were well protected inside the cabin. The pressure transducers had a range of $\pm$ 450 Pa and a resolution of 9.25 mV/Pa with an accuracy better than $\pm$ 0.5 Pa. Additional details describing the pressure system are provided by Fluck et al. (2010). All the transducers were pneumatically connected to a reference static pressure tube. The tube was 10 m long and the end of the tube was located inside a porous box in a cabinet inside the cabin, which assured that the air inside the box had negligible velocity. The reference static pressure (p_∞) was compared with the static pressures measured by Pitot-static probes fixed to a pole on the stern of the boat. The pole was approximately 2 m high and several Pitot-static probes were fixed onto it. The anemometers were deliberately pointed in different directions. All the static and the total pressures from the Pitot-static probes were connected to the transducers inside the cabin. When the boat was at the wharf, the pressure differences between p_∞ and the static pressures measured on the pole were found to be negligible, as expected. Conversely, the differences between the static pressures were larger while sailing. This was assumed to be the result of the influence of the sails on the static pressures measured on the pole. For this reason, the p_∞ was taken to be that measured inside the cabin and not by the probes on the pole.

Pressures were acquired at 100 Hz for 90 seconds. High-frequency fluctuations would have been damped by the long tubes (up to 20 m long) and hence a higher sampling frequency would have resulted in additional and redundant stored data.

Tests were performed on 2 different days but all the pressures hereby presented were measured the second day. The pressure transducers were calibrated before testing with the yacht at the dock. To take into account thermal effects, approximately every 20 minutes, the tests were interrupted and pressures were measured with the sail inside its bag in the yacht cabin. Thus, they were all at the same pressure as the reference pressure. These measured zeros were then subtracted from the signals measured during the actual tests, assuming a linear drift with time.

Pressures were measured using two different approaches. In the first case, pressures were measured with the yacht sailing in the most stable sailing state as possible with the sails in a fixed state of trim and the yacht on a constant course. Pressures were recorded and averaged over the sampling period. In the second case, pressures were measured while one sail condition was changed at a constant rate. For instance, over 90 seconds, the sail was trimmed in from fully eased to hard in. For these test cases, the pressures were averaged in sets of approximately 15-second duration and the resulting six averaged values were used to show the pressure variation with the sail trim.

2.3. Measuring the dynamic pressure

The dynamic pressure was measured with the Pitot-static probes fixed onto a pole on the stern of the yacht. The pole was mounted on the port side when pressures on the windward side of the sail were measured and on the starboard side when pressures on the leeward side of the sail were measured. The pole was also inclined at approximately 20° from the vertical axis of the yacht so that the Pitot-static probes were always leaning to windward from the yacht. Figure 3 shows the pole supporting the probes while sailing upwind after the tests.

A CFD analysis modeling an AC33-class yacht sailing downwind was performed. It showed that, in the region where the Pitot-static probes were located during the tests, the dynamic pressure is

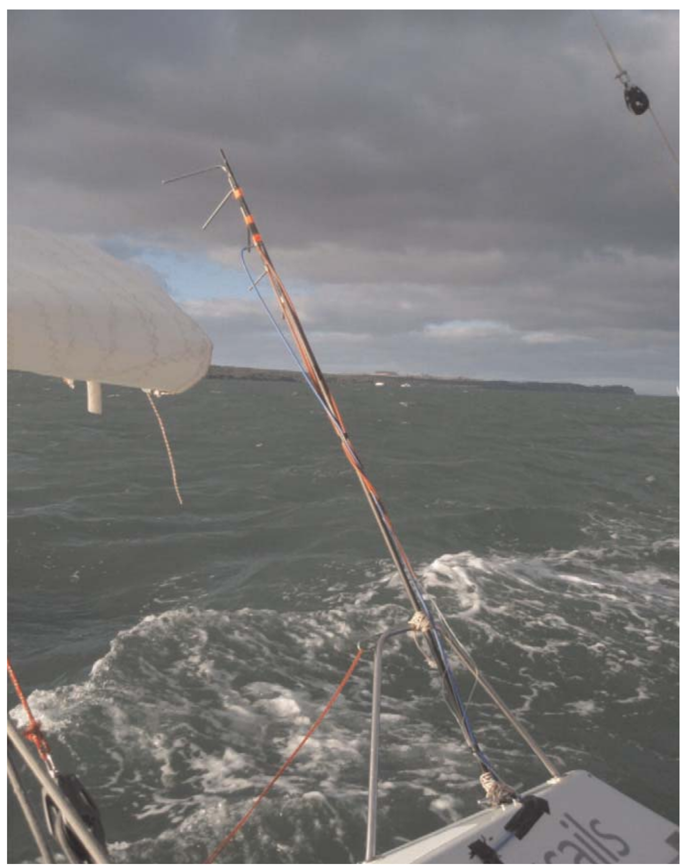

Fig. 3 Pole supporting the Pitot-static probes (shown while sailing upwind after the tests)

between 0% and 20% higher than in the far field. Conversely, 2 m above the head of the mast, the dynamic pressure is between 20% and 30% lower than in the far field. The consequence of this is that the pressure coefficients that have been presented may be up to 20% lower than they should be. Note that any error in the measurement of q_∞ will only affect the relativity between plots of say "max-eased" with "eased," because these were recorded at different times, whereas the data across each strip at a particular trim were recorded simultaneously, and a perturbation in q_∞ will affect all results in an identical way.

Initially, a single pivoting Pitot-static probe was mounted on the pole. In a previous experiment (Viola & Flay 2010b), in which pressures were measured on upwind sails, the wind was able to align the pivoting anemometer used with the wind direction. This setup was not appropriate for the present test, however, because the AWS was not high enough to align the anemometer into the wind. Therefore, three fixed Pitot-static probes aligned in different directions were used. The pressure differences from all three probes were measured at each acquisition and then the pressure measured by the Pitot-static probe aligned most favorably with the local wind direction (i.e., the one giving the highest reading) was used as the reference dynamic pressure q_∞. In the present article, q_∞ was between 4 and 40 Pa.

The AWA was measured with the standard on-board yacht instrumentation located at the top of the mast.

3. Results and Discussion

Figure 4 shows the Platu25-class yacht sailing with the pressure-tapped asymmetric spinnaker. In the full-scale AC33-class yacht, the top of the spinnaker is at the same height as the top of the mainsail. Therefore, the measurements were performed with the mainsail lowered (one reef was taken) from the hoist shown in Fig. 4, so that the heads of both sails were lined up during the measurements. As a consequence, the lower center of effort of the mainsail led to a heel angle of approximately 10°, which is lower than that shown in Fig. 4.

Fig. 4 The yacht and the pressure-tapped sail. The black bands show the locations of the pressure taps. The red bands were used by the VSPARS sail-shape recording system

Three AWAs and several sail trims were measured. The full-scale asymmetric spinnaker was designed to be sailed at approximately AWA = 80° in light air. The Platu25-class yacht does not have a very large righting moment, and therefore an AWA of 80° was a fairly tight angle to be sailed on such a yacht carrying a spinnaker without causing excessive heeling. This is because the lower the AWA, the higher the AWS, and therefore the higher the heeling moment. Two additional (larger) AWAs were tested, namely 120° and 170°.

The pressure signals were remarkably unsteady for the reasons discussed in the Introduction. It was found that the standard deviations of the pressure time histories were approximately 50% of their mean values. Indeed, this is not surprising, because the effective turbulence intensity of the AWS is probably in the region of 20% to 30%. In fact, it was not possible to keep a constant sail trim and to sail a constant course. When a gust arrived, the AWS increased and so did the heeling moment. The yacht began heeling and the helmsman reacted immediately to change the course to increase the AWA. The yacht then straightened up and accelerated as a result of the reduction in hydrodynamic resistance. The increased boat speed led to a lower AWA and the sail then had to be trimmed in. As soon as the gust passed by and the yacht slowed down, the sail became overtrimmed and it had to be eased. Therefore, the AWA and the sail trim were changing continuously. The frequency and the amplitude of the changes in the course and in the sail trim are certainly larger on small yachts such as the Platu25 class than on large yachts such as the AC33 class, and thus much care has to be taken in transferring the results obtained on a tender keel boat to a more stable large keel boat with a relatively much heavier keel.

The pressure measurements are presented in terms of a pressure coefficient (*Cp*), defined as the difference between the pressures measured by the pressure taps on the sail and the p_∞, measured inside the cabin, divided by the reference dynamic pressure (q_∞), measured by the selected Pitot-static probe on the pole. The pressure distributions presented have been smoothed to present general trends. The smoothing was done by fitting polynomials of various orders to the data, where the residual of each was less than 10% of the measured value.

3.1. General pressure distribution trends

Pressure distributions on sails can be explained in terms of classic aerodynamic theory for thin airfoils (e.g., see Abbott & Von Doenhoff 1949). In the midheight region, the flow direction can be considered mainly in the chordwise direction. If the local flow at the leading edge is tangent to the sail, then the angle of attack is called the ideal angle of attack (Theodorsen 1931). In this case, the stagnation point is at the leading edge, where the pressure is nearly equal to the stagnation pressure and $Cp \approx 1$. Downstream of the stagnation point, on both the sides of the sail, the pressure drops to lower values. On the leeward side, Cp decreases along the chord until about the maximum depth (draft) of the sail and then increases again until roughly $Cp \approx 0$ if there is no trailing edge separation or remains negative if there is trailing edge separation (Katz & Plotkin 2001). On the windward side, the flow speed is slower and the pressure is nearly constant with positive Cp for most of the chord length. At the trailing edge, the windward Cp decreases to match the leeward-side trailing-edge Cp.

If the leading edge presents a positive angle to the oncoming flow, a leading-edge separation bubble occurs (Katz & Plotkin 2001). The flow separates from the leeward side of the sail and reattaches again within the first quarter of the chord length. The pressure on the leeward side decreases abruptly near the leading edge and then increases until approximately the reattachment point. Further downstream, the pressure decreases again as a result of the sail curvature and then increases after the maximum sail curvature. This latter pressure increase can lead to trailing edge separation. If trailing edge separation occurs, the pressure recovery is interrupted and the pressure remains nearly constant and equal to the so-called base pressure. Figure 5 shows a schematic drawing of the flow field and the corresponding pressure distribution.

As long as the flow does not separate, the higher the angle of attack, and the higher the suction near the leading edge. At high angles of attack, the leading edge suction peak is much higher than the cambered-related suction peak and thus a second peak does not occur. When the flow separates and does not reattach downstream, the leading edge suction peak decreases. At very high angles of attack, higher than the separation angle, the pressure becomes almost constant and equal to the base pressure.

The stall angle on the midsection of an asymmetric spinnaker is above 20°. On an equally cambered two-dimensional section, the stall angle would be significantly lower. On three-dimensional sails, the tip vortices take a large amount of flow from the windward side to the leeward side, increasing the pressure on the leeward side. Therefore, the flow is able to reattach downstream at higher angles of attack. More details about the pressure distributions on downwind sails can be found in Viola and Flay (2009, 2010a).

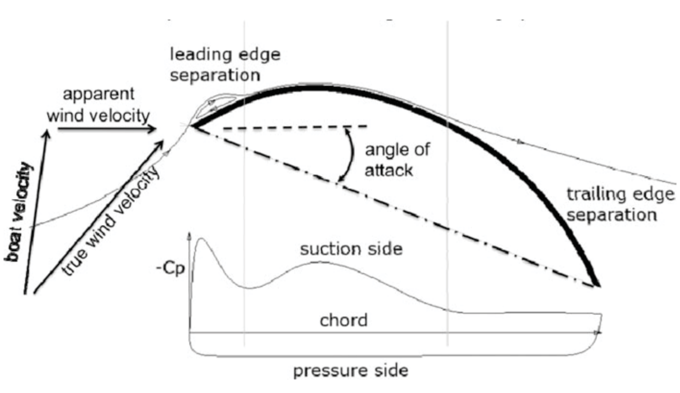

Fig. 5 Schematic drawing of the flow field and of the corresponding pressure distribution on a sail section

3.2. Pressure distributions from different trims

Figure 6 shows Cps on the leeward side of the three horizontal sections of the asymmetric spinnaker for AWA = 120°. Cps are plotted along the curve length for each sail section for four different sail trims. The sail is initially eased as much as possible (max eased trim in Fig. 6). The low angles of attack on the top sections of the sail thus lead to flapping of the leading edge. The pressures on the top section (three-fourths of the sail height) show that the sail is trimmed at the ideal angle of attack. On the lower sections, a leading edge suction peak occurs, and the Cp shows a suction peak within the first quarter of the sail. In the second half of the curve length, trailing edge separation occurs and the Cp becomes almost constant.

When the sail is trimmed in just enough to stop the luff from flapping (trim eased in Fig. 6), a leading edge suction peak occurs on the top section. Sailors would generally consider this to be the

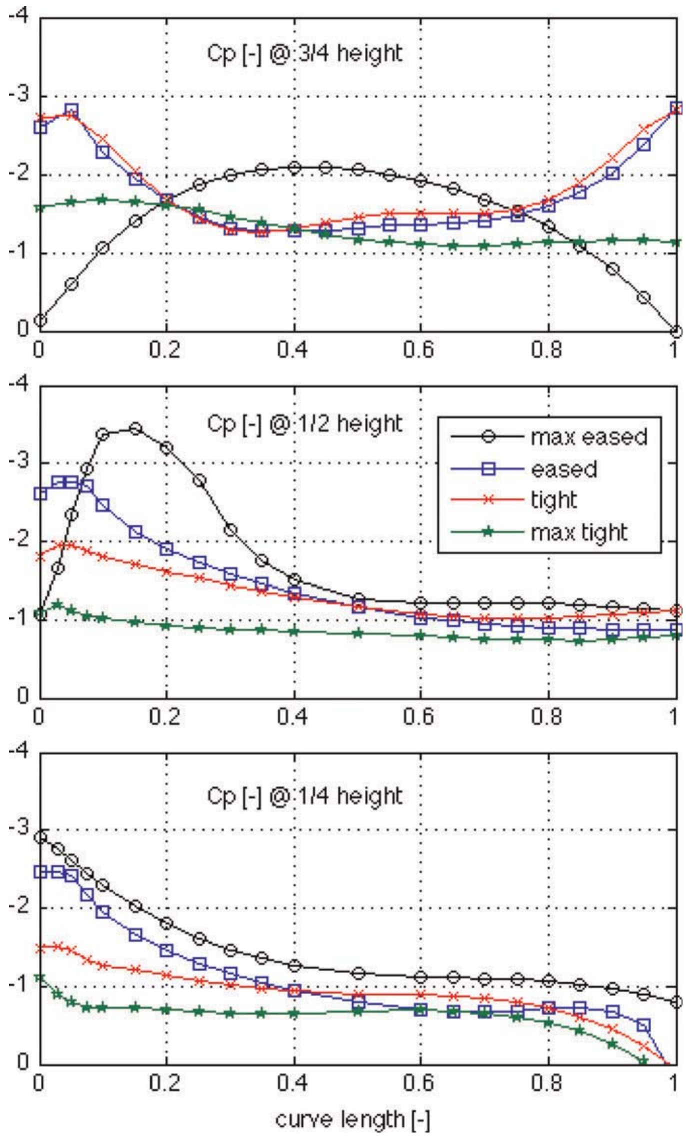

Fig. 6 Leeward pressure coefficient (Cp) on the three sail sections for four sail trims

optimum trim, i.e., the trim that produces the maximum boat speed. On the middle and bottom sections, the suction peak shows a decrease resulting from movement of the trailing edge separation point upstream along the curve length. On the top section near the trailing edge, Cp decreases down to -3 and shows a symmetrical distribution with respect to the centerline of the sail. These significant changes in pressure distribution across the top section of the sail with trim alterations are very interesting and are discussed in detail in the following paragraphs.

Figure 4 shows a photograph of the Platu 25 sailing at AWA = 80°, and it can be seen that the spinnaker pole is close to the forestay. For the results shown in Fig. 6 at AWA = 120°, the spinnaker pole was positioned further aft, and the spinnaker was further around in front of the yacht. It can be seen in Fig. 4 that the head of the spinnaker is very narrow, because it is a scaled-down shape designed for an IACC yacht sailing at AWA = 80°. Furthermore, as stated earlier, the pressure tests were carried out when the mainsail was reefed so that the heads of the spinnaker and mainsail were aligned, whereas Fig. 4 shows the mainsail at full height. According to the Platu 25 class rules, the mainsail girth length at three-fourths height is 1380 mm. This results in an angle of approximately 30° at the mainsail head, which is quite low, i.e., it has a rather "pointed" head with not much area near the top. This means that in downwind sailing, the mainsail will have much less impact on the behavior of the spinnaker than a "flat-head" main would. Thus, in the following discussion regarding the pressure distributions at the top of the symmetric spinnaker, the effect of the mainsail is ignored, because it is expected to be small.

It is known that a so-called delta wing such as used on the supersonic Concord aircraft produces high lift by having separated flows off both swept-back edges, producing strong spiralling vortices, e.g., see Hummel (2006). These vortices produce strong three-dimensional flow, which can cause a wing to exhibit high values of lift coefficient at high angles of attack, because they bring flow downward onto the central section of such delta wings. For example, the 65° delta wing in Hummel (2006) at an angle of attack of 13° has pressure coefficients as low as -2.5 at 20% of the chord downstream of the apex. The highest suction is at the edge, and the lowest suction is in the center and is approximately -0.2. Further downstream the highest suctions move away from the edge, as the pair of vortices grow, and their centers move further inboard from the edges. Such behavior is not confined to high-speed, low-turbulence aerodynamic flows. Conical vortices resulting in separated flows with low pressures have also been observed above the roofs of buildings emanating from a corner when the wind is at an oblique angle to the edge discontinuity, e.g., see Ginger and Letchford (1993).

It has been observed that sails can also exhibit such "delta wing-type" behavior (Bethwaite 2003). Bethwaite states "The head of a spinnaker which is trimmed to float more horizontally than vertically at its head can and should develop these roll-over vortices."

The authors believe that the pressure distributions shown at the three-fourth height section of the spinnaker in Fig. 6 for AWA = 120° for the trims of eased and tight are exhibiting such delta-wing characteristics and that this is the first time they have been measured on a yacht sail. The apparent wind direction for these measurements would have been aligned approximately with the bisector of the apex (head) of the spinnaker. This kind of pressure distribution is expected to be caused by flow that was separating off both sides of this "delta wing-like" spinnaker head shape and thus producing a pair of strong vortices, which cause the low pressures at the sail edges. At lower heights, the orientation of the spinnaker becomes more vertical and the angle would have been too large to allow these vortices to remain attached to the upper surface and so they would have left the sail surface, which is why the pressure distributions are more conventional at lower spinnaker heights. Also, the AWA changes with height, giving an onset flow to the sail, which is more aft near the head and more on-the-beam at the foot. This effectively changes the angle of attack with height, bringing the flow onto the spinnaker leading edge (luff) at the lower heights.

At the three-fourths height section, the "max-eased" trim would have allowed the flow at the head to come onto the sail more along the luff, thus enabling the sail to work in a more conventional manner at its ideal angle of attack as mentioned previously. In the "max tight" trim, the spinnaker head flattens and takes up a more vertically orientated setting so that the separated flow is unable to generate vortices that remain along the lee surface, and so the spinnaker shows the conventional uniform low pressures that are found in the disturbed wake behind bluff bodies.

On the windward side (Fig. 7), Cp is almost independent of the sail trim and, therefore, only Cp measured at the optimum trim is shown. Along the chord length, Cp decreases only near the trailing edge, where it is adjusting to match the Cp on the leeward side. Because the pressure tap closest to the trailing edge was approximately 100 mm from the trailing edge, the last measured Cp on the leeward side is not equal to the last measured Cp on the windward side.

3.3. Pressure distributions for different apparent wind angles

Figure 8 shows Cps on the leeward side of the three horizontal sections of the asymmetric spinnaker for apparent wind angles of 80°, 120°, and 170°. The sail was retrimmed to the optimum trim at each AWA. On the top section, when sailing at AWA = 120°, the Cp shows the delta wing-like trailing edge suction. It should be noted that this trailing edge suction does not occur at AWA = 80° because for this apparent wind angle, the wind is onto the spinnaker luff. At AWA = 170°, the wind is almost from directly aft with the spinnaker in front, and the top section of the sail is behaving as a flat plate with a disturbed wake flow resulting in uniform pressure distribution.

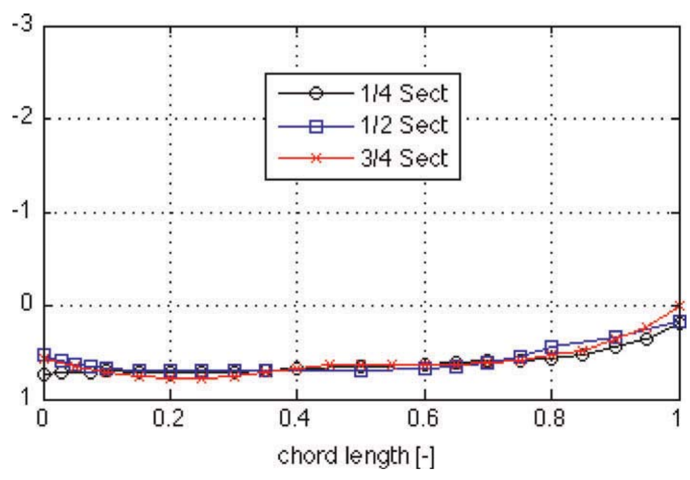

Fig. 7 Windward pressure coefficient (Cp) on the three sail sections

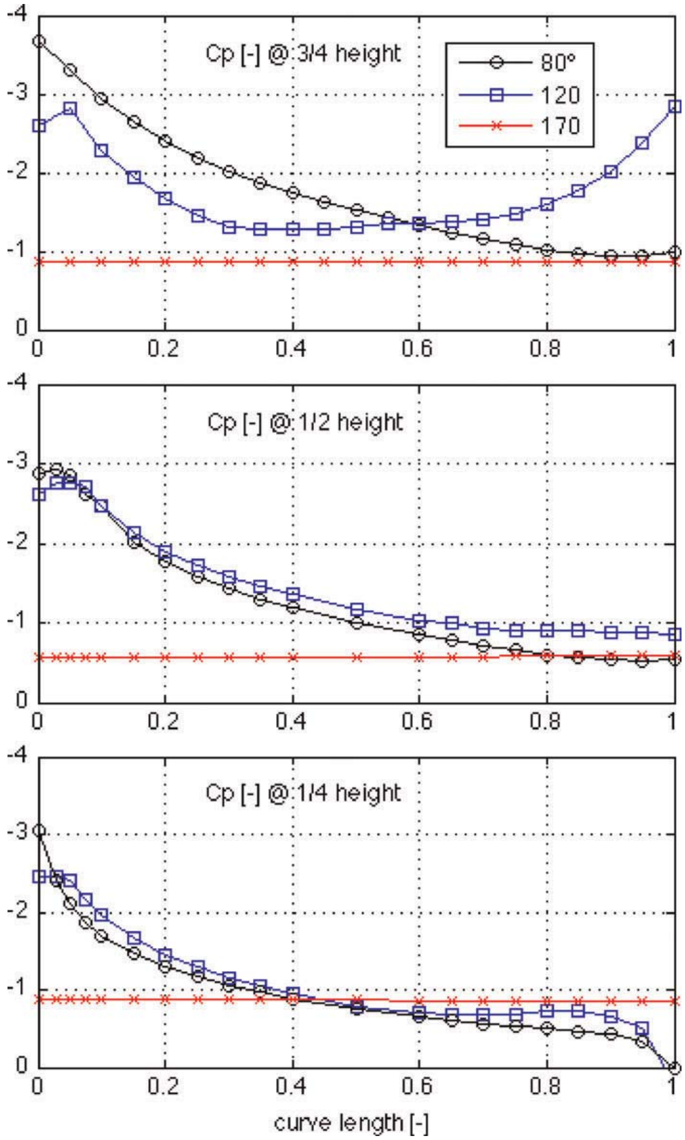

Fig. 8 Leeward pressure coefficient (*Cp)* on the three sail sections for apparent wind angles (AWAs) of 80°, 120°, and 170°

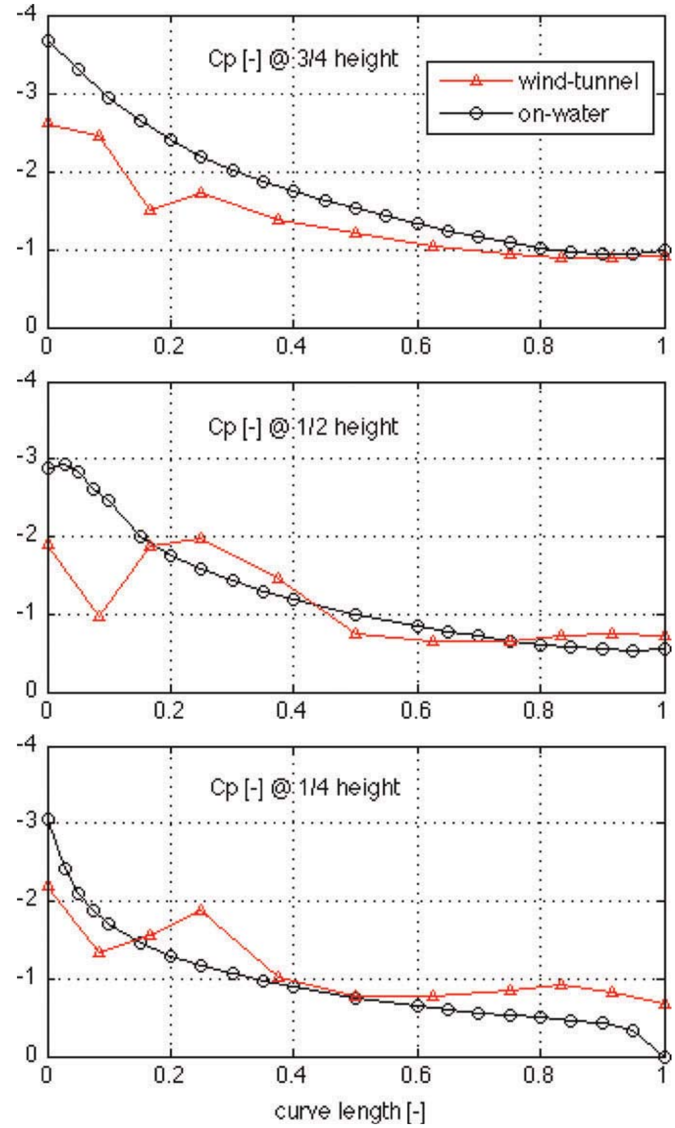

Fig. 9 Wind tunnel and on-water leeward pressure coefficients (*Cp*s) on the three sail sections for apparent wind angle (AWA) = 70° and 80°, respectively.

Figure 8 shows that the sail can be trimmed at AWA = 80° and AWA = 120° to achieve high suction on the entire leeward side of the sail. Conversely, when the AWA is increased further, the sail cannot be eased sufficiently and stall occurs. Along each section, the pressure was observed to oscillate around a nearly constant mean value. The integral of *Cp* along the curve length represents most of the aerodynamic force resulting from the sail. Figure 8 thus indicates that the aerodynamic force is decreased when stall occurs.

The *Cp*s on the windward side are not presented here because they do not show any significant differences from the *Cp* trends evident in Fig. 7.

3.4. Full-scale and wind tunnel comparison

Figure 9 shows *Cp*s on the leeward side of the three horizontal sections of the asymmetric spinnaker measured on the water and in the wind tunnel. *Cp*s were measured on the water for the optimum trim at AWA = 80°. Wind tunnel measurements were performed with a 1/15th model-scale flexible sail at the optimum trim at AWA = 70°. A detailed description of the wind tunnel measurements can be found in Viola and Flay (2009, 2010a).

Figure 9 shows good agreement and similar trends between the *Cp*s measured in full scale and in the wind tunnel. The *Cp*s measured in full scale show only one suction peak near the leading edge. Conversely, the *Cp*s measured in the wind tunnel show two suction peaks, the first one being near the leading edge and the second one being near 25% of the curve length. When the angle of attack is increased, which can be the result of a tighter trim or to a higher AWA, it has been observed that the leading edge suction peak is increased, whereas the curvature-related suction peak is decreased. Therefore, the differences between the full-scale and the wind tunnel pressure distributions in Fig. 9 suggest that the three sail sections tested in full scale experienced higher angles of attack than the three sail sections tested in the wind tunnel. In fact, as shown by Viola and Flay (2010a), different AWAs lead to small differences in the pressure distributions, whereas larger differences are measured for different trims. A tighter trim is thought to have been used in the full-scale measurements as a result of having to trim in the unsteady wind conditions. Conversely, the stationary wind conditions and fixed yacht model attitude in the wind tunnel allowed a more eased trim to be used.

Also, it is known that the pressure recovery between the two suction peaks is correlated with the reattachment of the laminar separation bubble. Therefore, the differences between the full-scale and wind tunnel pressure distributions could be the result of the absence of the laminar separation bubble during the full-scale experiment. It should be noted that the wind tunnel tests were carried out in uniform untwisted flow with a lower turbulence intensity (approximately 3%) than in full scale (estimated to be approximately 20%). Hence, the formation of a leading edge separation bubble would be more likely in the wind tunnel with its lower turbulence intensity, and also at the lower Reynolds number, which is approximately one-tenth of that at full scale. However, the authors consider that it is more likely that the differences in pressure distributions are the result of different sail trims rather than Reynolds number effects or to different turbulence characteristics of the flows.

Note also that as stated previously, the full-scale data were smoothed by fitting polynomials of various orders to the data, and this may have inadvertently smoothed out some of the variations that are evident in the wind tunnel data, which were not smoothed in this manner, because these results were much less variable.

4. Conclusions

Pressure distributions on sails have been measured only rarely. In particular, on-water pressure measurements have been performed only in upwind sailing conditions. As far as known by the authors, the present article presents the first full-scale pressure measurements on sails flown in downwind sailing conditions. Although numerical modeling and wind tunnel experiments neglect or model relatively poorly the unsteadiness of the wind, the movement of the sails and the yacht, on-water sail tests automatically take them into account.

Pressures were measured using 63 pressure taps distributed along three horizontal sections at one-fourth, half, and three-fourths of the sail height on an asymmetric spinnaker. The sail was designed for Emirates Team New Zealand, a possible challenger for the 34th America's Cup, when it was expected to be sailed with AC33-class yachts. Pressure distributions were measured for several sail trims and three AWAs on both the leeward and windward sides of the sail.

The main conclusions that can be drawn from the experiments are summarized subsequently.

4.1. Pressure distributions for different trims

- For the optimum sail trims, the Cp on the leeward side of the sail near the leading edge has a suction peak between $Cp = -3$ and $Cp = -4$, and downstream, Cp increases monotonically.
- On the windward side, Cp is almost constant and is slightly less than 1. Cp decreases near the trailing edge to match the leeward-side trailing-edge suction.
- In some trim conditions, the suction increases toward the trailing edge on the top leeward section only. It is argued that this is evidence of delta wing-like vortex formation on the top section of the spinnaker.
- Trimming-in the sail causes the leading edge suction to decrease as a result of trailing edge separation until Cp becomes almost constant and equal to –1 when stall occurs.

4.2. Pressure distributions for different apparent wind angles

- Almost the same pressure distribution is achieved by retrimming the sail for AWA $= 80°$ and AWA $= 120°$. Conversely, at higher AWAs, it was not possible to ease the sail enough and stall occurred. Therefore, Cp is almost constant and equal to -1.
- On the windward side, Cp is almost constant at each chordwise position, between 0 and 1, and decreases near the trailing edge to match the leeward-side trailing-edge suction.

4.3. Full-scale and wind tunnel comparison

- The full-scale and wind tunnel pressure measurements showed very good agreement in their trends.
- The pressure recovery on the lee side of a spinnaker is related to the leading edge reattachment mechanism. A second suction peak was visible in the first quarter of the curve length for the wind tunnel measurements, but in the full-scale measurements, any leading edge bubble was very small, and so the pressure distribution did not have a second peak, and the suction decreased monotonically toward the trailing edge.

Acknowledgments

We acknowledge the support of the staff and students in the Yacht Research Unit, and in particular, we are grateful to Mr. Baptiste Watier and Mr. Etienne Gauvain for their passion and support in managing and performing the on-water and wind tunnel experiments and Mr. David Le Pelley for his helpful advice. We also acknowledge the contribution of Dr. Nick Velychko in building and supporting the multichannel pressure system.

REFERENCES

Abbott, I. H., and Von Doenhoff, A. E. 1949 *Theory of Wing Sections,* Dover Publications Inc., New York, NY.

Bethwaite, F. 2003 *High Performance Sailing,* Adlard Coles Nautical, London, UK.

Braun, J. B., and Imas, L. 2008 High fidelity CFD simulations in racing yacht aerodynamic analysis, *Proceedings,* 3rd High Performance Sailing Yacht Conference (HPYDC3), pp. 168–175, December 2–4, Auckland, New Zealand.

Flay, R. G. J., and Millar, S. 2006 Experimental consideration concerning measurements in sails: wind tunnel and full scale, *Proceedings,* 2nd High Performance Yacht Design Conference (HPYDC2), February 14–16, Auckland, New Zealand.

Fluck, M., Gerhardt, F. C., Pilate, J., and Flay, R. G. J. 2010 Comparison of potential flow based and measured pressure distributions over upwind sails, *Journal of Aircraft,* **47,** 6, 2174–2177.

Gaves, W., Barbera, T., Broun, J. B., and Imas, L. 2008 Measurements and simulation of pressure distribution on full size scales, *Proceedings,* 3rd High Performance Yacht Design Conference (HPYDC3), December 2–4, Auckland, New Zealand.

Ginger, J. D., and Letchford, C. W. 1993 Characteristics of large pressures in regions of flow separation, *Journal of Wind Engineering and Industrial Aerodynamics,* **49,** 1–3, 301–310.

Hochkirch, K., and Brandt, H. 1999 Full-scale hydrodynamic force measurement on the Berlin sailing dynamometer, *Proceedings,* 14th Chesapeake Sailing Yacht Symposium (14CSYS), SNAME, pp. 33–44, January 30, Annapolis, MD.

Hummel, D. 2006 The second international Vortex Flow Experiment (VFE-2): objectives and first results, *Institution of Mechanical Engineers, Part G: Journal of Aerospace Engineering,* **220,** 6, 559–568.

Katz, J., and Plotkin, A. 2001 *Low-Speed Aerodynamics,* Cambridge University Press, Cambridge, UK.

Masuyama, Y., and Fukasawa, T. 1997 Full-scale measurements of sail force and validation of numerical calculation method, *Proceedings,* 13th Chesapeake Sailing Yacht Symposium (13CSYS), SNAME, pp. 23–36, January 25, Annapolis, MD.

Milgram, J. H., Peters, D. B., and Eckhouse, D. N. 1993 Modeling IACC Sail Forces by combining measurements with CFD, *Proceedings,* 11th Chesapeake Sailing Yacht Symposium (11CSYS), SNAME, pp. 65–73, January 29–30, Annapolis, MD.

Puddu, P., Erriu, N., Nurzia, F., Pistidda, A., and Mura, A. 2006 Full scale investigation of one-design class catamaran sails, *Proceedings,* 2nd High Performance Yacht Design Conference (HPYDC2), February 14–16, Auckland, New Zealand.

Theodorsen, T. 1931 "On the Theory of Wing Sections With Particular Reference to the Lift Distribution", *NACA Report, no. 383*.

Viola, I. M. 2009 Downwind sail aerodynamics: a CFD investigation with high grid resolution, Ocean Engineering, 36, 12–13, 974–984.

Viola, I.M., And Flay, R. G. J. 2009 Force and pressure investigation of modern asymmetric spinnakers, *International Journal of Small Craft Technology, Trans. RINA,* 151, B2, 31–40; discussion in *Trans. RINA,* 152, B1, 51–53.

Viola, I. M., and Flay, R. G. J. 2010a Pressure distribution on modern asymmetric spinnakers, *International Journal of Small Craft Technology, RINA,* **152,** B1, 41–50.

Viola, I. M., and Flay, R. G. J. 2010b Full-scale pressure measurements on a Sparkman & Stephens 24-foot sailing yacht, *Journal of Wind Engineering and Industrial Aerodynamics,* **98,** 12, 800–807.

Viola, I. M., Pilate, J., and Flay, R. G. J. 2011 Upwind sail aerodynamics: a pressure distribution database for the validation of numerical codes, *International Journal of Small Craft Technology,* **153,** B1, 47–58.

Viola, I. M., and Ponzini, R. 2011 A CFD investigation with high-resolution grids of downwind sail aerodynamics", *Proceedings,* Developments in Marine CFD, RINA, March 23–24, London, UK.

Warner, E. P., and Ober, S. 1925 The aerodynamics of yacht sails, *Proceedings,* 3rd General Meeting of the Society of Naval Architects and Marine Engineers, November 12–13, New York, NY.

Watier, P. B. 2010 "Comparison of full-scale and model-scale measurements of the aerodynamics of an asymmetric spinnaker", MEng Thesis, DTU Mechanical Engineering, Technical University of Denmark, Denmark, and Yacht Research Unit Report, The University of Auckland, New Zealand.

Wright, A., Claughton, A., Paton, J., and Lewis, R. 2010 Offwind sail performance, prediction and optimisation, *Proceedings,* 2nd International Conference on Innovation in High Performance Sailing Yachts (INNOV'SAIL), June 30–July 1, Lorient, France.

Discussion

Kevin Borrows, Visitor

I strongly agree with the authors' background and discussion of the strengths and weaknesses of respective sail testing methods, be that CFD, wind tunnel testing or full scale testing. Even in the relatively resource plentiful world of the America's Cup we struggle with the trade-off between CFD throughput and accuracy (Panel codes vs. RANS vs. LES/DES). Luckily this has become much less of an issue while researching AC72 Catamarans where the boats are sailing at AWA < 25 both up and downwind allowing for good global force prediction and therefore velocity prediction from panel methods. However, full scale empirical testing is still the preferred method of validation.

I think the authors' experimental method was sound and the assumptions (such as the negligible effect of the pin head mainsail and an assumed effect on dynamic pressure acquisition based on the effect on the flow field from CFD computations) were logical and fair.

I note in the caption of Fig.4 the yacht was configured with a sail shape measurement system. I believe documenting of the sail's shape—primarily camber and twist (AOA when combined with yacht AWA)—would have been useful in further evaluating the authors' findings. This is especially pertinent when the authors report that the biggest effects on Cps were trim related - orientation of the sail's sections with a measured AOA.

It is hypothesized that at certain AWAs the sail's upper section pressure distribution exhibits delta wing like characteristics – certainly the pressure distributions would lend themselves to this conclusion. Again what would be very useful for the purpose of further validation would be to compare the sail's flying shape at the "delta wing" sections to the measured onset flow (yacht's AWA at mast head). Knowing the "expected" AOA where the top of the asymmetric spinnaker was exhibiting delta wing-like characteristics, the reader could identify a range of sail trims where they may see this increased leeward side trailing edge suction and thereby describe the testing conditions (either wind tunnel or full scale) for secondary validation.

The comparison with wind tunnel data makes sense – and I agree with the conclusions for the expected differences. Again the onset flow of the sail's sections (numerical description of the trim) from the wind tunnel and full scale experiment would be helpful.

Patrick Bot, Visitor

First of all, I would like to thank SNAME and the authors for giving me the opportunity to discuss this very interesting paper.

The authors present an original study of full-scale tests where pressures have been measured on a downwind sail for several wind angles and sail trims and compared to model scale tests in a wind tunnel. Such measurements are very useful to better understand the flow around a downwind sail and to assess the validity of numerical and model-scale studies to model the real situation of sailing. The paper clearly highlights the difficulties of on-water testing on a sailing yacht, due to the complex environment and the numerous uncontrolled parameters in actual sailing conditions. Considerable difficulties arise to determine the sailing conditions, to calibrate sensors and to cope with all perturbations. Most of the parameters are inter-dependent, rather unsteady, and not controlled. The onset flow is difficult to determine (atmospheric boundary layer, turbulence, apparent wind twist, on-board measurement perturbed by sails and yacht motion, etc.). Hence, comparing full-scale tests with model scale or numerical results is very challenging. For all these reasons, the remarkable work presented in this paper must be acknowledged as a considerable contribution. I would just moderate the statement from the authors of a "very good agreement" between full scale and wind tunnel pressure measurements which sounds to me a little bit too optimistic, regarding Figure 9 and the differences between full scale and wind tunnel testing conditions, (for example different AWA, trim, wind twist).

The authors emphasize the high level of unsteadiness of the results (standard deviation 50% of mean value) due to the onset flow turbulence and the impossibility to keep a constant course and sail trim. The presented data are averaged in time, and smoothed in space by fitting polynomials to present general trends. We may wonder how this data processing and the necessary limited spatial resolution affect the real pressure distributions, which may undergo strong gradients.

The observation of a delta wing-like behaviour on the highest sections is also interesting. This appears to be related to the local onset flow hitting the sail head first. Further investigation would allow more interpretation to be derived. It may be useful to determine if this is a singular characteristic of the studied case, or if it is a more general behaviour of the top of a downwind sail. In fact, some specific features of this particular case may favour the delta wing-like behaviour, such as using the sail at a greater AWA (120°) that it was designed for (80°), and the very narrow mainsail head at the same height as the spinnaker head when the main is reefed. At AWA=170° where this behaviour was not observed, how was the pole trimmed? Is a delta wing-like behaviour recovered when the pole is trimmed more aft and high, as would be the case with a symmetric spinnaker?

It should be highlighted that the authors and the Yacht Research Unit (YRU) of the University of Auckland have put a great deal of continuous effort in sail pressure measurements, both in a wind tunnel and at full scale on the water. They have been pioneers on this track and have obtained remarkable success. In this paper, the authors used single-sided pressure taps on the sail with tubes to convey the pressures down to transducers located inside the yacht cabin. This method not only requires handling numerous long tubes along the sails, but also necessitates the reference static pressure to be determined, which proves to be difficult, as shown by the authors. Further developments in the YRU led to a different system based on differential pressure transducers directly on the sail [Le Pelley et al. 2012, Motta et al. 2013], which seems easier to handle and promising for further full-scale pressure measurements.

Again, given the difficulties to run on-water full-scale measurements, and particularly on downwind sails, this work is a remarkable contribution to improve the knowledge of sail aerodynamics. This also shows that there is still a lot to investigate on these tricky flows, both in real sailing conditions and in more controlled situations.

ADDITIONAL REFERENCES

LE PELLEY, D. J., D. Morris, P.J. Richards (2012). Aerodynamic force deduction on yacht sails using pressure and shape measurement in real time. 4th High Performance Yacht Design Conference. Auckland, New Zealand.

MOTTA, D., Flay, R.G.J., Richards,P.J., Le Pelley, D.J., (2013). An Experimental Investigation of Asymmetric Spinnaker Aerodynamics Using Pressure and Sail Shape Measure-ments. 3rd International Conference on Innovation in High Performance Sailing Yachts, INNOV'SAIL, Lorient, France.

Vincent Chapin, Visitor

The first perception of the paper has been that guys who have done these "on-water measurements" are courageous guys because it should not be easy to do and to learn from that job, as it seems a complex job with a lot of uncertainties related to measurement techniques, hypotheses, and environmental variations. Also the first question that came to mind is to know if "The game is worth the candle".

The technical problems of on-water measurements are described and the authors show that they are aware of these problems and the related inaccuracies and difficulties of separating sources of inaccuracy. Key accuracy numbers are evocated rather than precisely defined or estimated. It is explained that the pressure transducer used has 1Pa of accuracy, which implies 10% accuracy on the velocity and 20% on the pressure. Error bars may be helpful on Cp distribution to increase the relevance of analysis and comparisons between on-water and wind tunnel measurements.

One key difficulty, the measurement of a reference static pressure, is described in detail and the solution used is defined. It is measured in the cabin for the numerator and outside on the pole at 2 meters high in the wake of the mainsail for the denominator of the pressure coefficient. The dependence of the reference static pressure to the environment is described in the paper but no measurements of these variations are given. Would it be possible to validate the principle or quantifying variations with sailing conditions through a wind-tunnel experiment?

This is probably one of the main questions about this paper to be able to characterise physical phenomenon with sufficient accuracy to inspire better sail design.

Some questions or remarks about a few details in the text are given below:

Question: in Section 1.3 On-water tests:

What is considered into "dynamic effects" because many things may be considered? This may be clarified. I am not sure that Viola (2009) is the right reference in the following sentence: "A review of potential flow and RANS applications is presented in Viola (2009)". Moreover, there is an ambiguity because there are 2 references Viola (2009) in the paper.

Some typographic errors: Gaves or Graves, Broun or Braun? In this section it seems useful to say few words about pressure variations with altitude in the atmospheric boundary layer.

Comments on Section 3: Results and Discussion:

1. It is interesting to have on-water pressure measurements on sails but it would be useful to have corresponding flying sail shapes to make comparisons with wind-tunnel tests or numerical simulations. Have they been measured during tests? Angle of attack and sail camber estimations in the three measured sections would be meaningful to understand pressure distributions.
2. The difficulty of these measurements in a real environment with wind gusts, AWA changes, and boat acceleration is well illustrated and raises the question of the usefulness of these measurements. What do they aim at?
3. Can the principle of pressure coefficient Cp calculation based on two different static pressure measurements in the cabin and in the pole be validated in a wind-tunnel experiment?
4. Section 3.4 Full-scale and wind tunnel comparison: It seems that the pressure coefficient comparisons between wind-tunnel tests and on-water tests is misleading because smoothing is applied for on-water measurements but not or not in the same way on wind-tunnel tests. Is that the case?

One more general comment is that the paper makes comparisons between model scaled tests in a wind tunnel and full-scale tests on-water without speaking of the differences of elasticity of materials used for sails. This might be developed in few words.

In conclusion, the paper was very interesting to read and stimulating for future research projects and in the field.

Professor Fabio Fossati, Visitor

As I'm not a member of the Society, I deeply appreciate the honor of having been asked to discuss this interesting paper.

The authors should certainly be congratulated by all interested in sailing yacht research for their investigations: sail aerodynamics is commonly investigated by using wind tunnel testing and numerical methods and both methods have various drawbacks. Full scale testing certainly represents a valuable approach to validate results from these methods; moreover full scale testing allows the investigation of sail performance in real sailing conditions and my personal vision is that global aerodynamic forces measurements combined with simultaneous sail pressure distribution and sail shapes measurements at full scale level are of paramount importance for the development of downwind sails and their performance understanding.

Several full scale sail pressure measurements have been carried out in recent years, as reported in the paper's references list, and all previous attempts highlighted the well known difficulties in carrying out pressure measurements at full scale.

This paper presents the first full-scale pressure measurements on an asymmetric spinnaker and results are compared with the same measured data obtained by means of wind tunnel tests; in particular this comparison shows very interesting differences in the pressure distribution especially near the leading edge points.

So I would like to try to address the discussion from the angle of the experimental pressure measurements carried out by the authors to investigate sail aerodynamics at full scale as well as from the angle of the differences outlined moving from the wind tunnel testing at scale model towards full scale scenario.

The main point which would require a better explanation is the following: concerning the wind tunnel measurements the authors highlight two suction peaks in the Cp distributions, while at full scale the pressure distribution does not have the second peak. In my opinion these differences are mainly due to Reynolds effect and in particular to the critical Reynolds number transition occuring from the model scale to the full scale conditions.

However, the spatial definition used to detect the pressure distributions seems to be too poor to well identify the two peaks. Are other data available to confirm this observation?

The above mentioned differences could also be related to differences in sail shape and from this point of view it would be interesting to know what the weight of pressure taps and tubes are and, if in the authors' opinion, they may affect the sail shape at full scale. Was the sail shape detected during the on-water tests?

Another interesting discussion point is related to the damping effects on the high frequencies in the pressure measurements due to the long tubes used, as mentioned by the authors. Was the measurement system tested in order to define the transfer function of the tubes? Was a frequency analysis performed on the pressure measurements to verify their harmonic content? This could be useful to understand if the very high reported values of the standard deviation (50%) can be related to the wind or to some noise that can affect the measurement chain. In particular the fluctuation of the tubes together with the sail or in the pockets can introduce some dynamic effects on the pressure measurements and this should be better highlighted.

With reference to the pressure distribution results, are the presented Cp values the mean values of the coefficients? Why did the authors decide to smooth the pressure data? Why has a polynomial law been used? In my opinion it would be more convenient to show the actual data eventually superimposed to an interpolation.

In order to have a better understanding of the differences in the pressure distribution between full scale and model scale, another issue which could be better clarified is related to thermal effects: which kind of thermal effects make necessary the zero procedure described in the paper? Which part of the measurement chain is affected by the mentioned thermal effects? Have the authors to face this only at full scale or even in the wind tunnel experiments?

The final point which could be better clarified is related to the dynamic pressures measured by the pitot tubes on the pole: are these values related to the static pressure measured in the cabin? The static pressures measured on the pole by the pitot tubes probably cannot be considered reliable because of the yacht displacements under sailing.

In conclusion, I wish to again thank the authors for their interesting paper and I underline that the above mentioned discussion points and remarks are meant for amplification and clarification purposes, hoping they may be of assistance in leading further experimentation into the proper channels.

Peter Heppel, Visitor

Overall comment: This paper reports a much-needed experiment in a clear and objective way. The experiment sheds new light on the flow structure created by these sails.

Some detailed comments follow:

Section 1.1:
While sails might be expected to have an attached boundary layer over much of the surface, in practice many boats perform better upwind in configurations that result in large regions of separated flow. The IACC V5 is a notable example.

Section 1.2 Wind tunnel tests:
It is at least as important to scale the membrane elasticity as it is the self-weight.

Jackson (Ontario, 1981) provided a good discussion on scaling of aeroelastic membranes in steady-state. He suggested a parameter (structural stiffness / aero stiffness), which for extensional modes can be shown to be equivalent to the membrane strain. (PH, unpublished)

Membrane structures deform inextensionally (i.e. without change of strain) as well as extensionally. The ratio of aero stiffness to inextensional stiffness is independent of windspeed and scale for a given geometry. (PH, unpublished)

Light downwind sailcloth has mass ~40 gsm and hence weight ~ 0.4 N/m^2. In the present case the dynamic pressure is 2.4 to 10 Pa. Thus the self-weight is significant at 2 m/s but not at 4 m/s. If the same material is used at model scale and at full-scale, then for correct scaling of elasticity, the dynamic pressure should scale with 1/(Dimension).

Section 2.2
The reference pressure is the internal cabin pressure. While it's difficult to imagine a better place, the cabin pressure will be influenced by the size and disposition of the openings. For example, If there is just one opening facing the wind the cabin pressure will be above the free-stream static pressure.

It would be good to discuss the influence of the limited sensitivity of the pressure sensors (0.5 Pa) on the accuracy of the plots of pressure distribution.

Section 2.3
Measuring AWS and AWA is notoriously difficult because of the influence of the vessel itself on the near flow field. In this experiment, it was more important to have a good AWS measure, because it is used to normalize the results, than the AWA measurement which is only used to categorize the sailing condition. Thus the use of the on-board yacht system for AWA is reasonable. But it would be comforting to see more testing to justify the AWS measurement calibration (+0% to +20%)

Section 3
Unsteadiness and ambient turbulence. The authors have correctly identified the effect of the boat's velocity in magnifying the free-stream turbulence. However, with turbulence it is important to consider its scale: in the atmospheric boundary layer the free-stream turbulence may indeed be around 20% . But there is a spectral peak at about 1 minute which corresponds to a length-scale of a few hundred metres, and corresponds to the gusts described here.

It would be good to see the spectra of the pressure traces, corrected for resonance in the tubing. Compared with the expected free-stream spectrum this would give an indication on which parts of the signal were due to free-stream turbulence. Further, it might be assumed that any strong peaks in the 0.1-10 second range are due to other actions such as structural or archimedean vibration, or wave excitation. There are many discussions on this in the field of building aerodynamics. See for instance the extensive publications of Lawson or Davenport.

Section 3.1
It would be more appropriate to compare the stall angle for a wing of the same aspect ratio, rather than that of an infinite wing.

Section 3.2, 3.3
Fig. 6 is the most interesting result, and especially the variation with trim at ¾ height. It is impressive to see the recognition that the leading-edge separation is better considered a vortex shedding. But I don't understand how there can be a trailing-edge Cp of -3 on the upper side and not on the lower side. Perhaps the authors could show some pressure distributions from the literature of delta wings?

Section 3.4
Was any flow-visualization done to back up the interpretation of Fig. 6?

William C. Lasher, Member

I appreciate the opportunity to comment on this very interesting paper. As you state this is the first measurement of pressure distributions on a full-scale spinnaker to be reported in the literature. This is a significant contribution to our understanding of spinnaker aerodynamics. It is clearly a difficult measurement under complex flow conditions, and the experimental approach you have taken to deal with these complexities is appropriate.

The ability to differentiate between what happens on the water and what happens in a wind tunnel (or CFD simulation) is becoming increasingly important as design and analysis methodologies advance. In order to make reasonable comparisons between full-scale data and that from a wind tunnel experiment or CFD simulation, it will be necessary to both minimize and estimate uncertainty. Based on the results shown in Figure 9 (comparing the full-scale data with the wind tunnel data), it appears that your approach to measuring free-stream dynamic pressure and the reference pressure is sound; however, there is no discussion about the differences in sail shape. The caption for Figure 4 implies that sail shape was recorded but no information on this is reported. Did you in fact measure the sail shape? If so, could you discuss the differences in sail shape between the full-scale tests and wind tunnel experiments? I would also be interested in your thoughts as to what should be done in the future to both minimize and estimate total experimental uncertainty for this problem.

My second question relates to the optimum trim, which you state as being the "eased" trim. In Figure 6 it looks like the integrated pressure (at least on the lower 2 sections) would be higher using the "max eased" trim rather than the "eased" trim. Since the AWA in this case is well behind the beam, this suggests that the "max eased" trim would produce a higher driving force than the "eased" trim. Would you be able to integrate the pressure over the sail surface, or at least comment on this?

Yutaka Masuyama, Member

I would like to congratulate the authors on the developing a measurement system of pressure distribution on a full scale downwind sail and describing the valuable measured data. I think this is the first report which shows the measured pressure distribution on the full scale downwind sail by on-water tests and points out the differences of pressure distribution between full scale and scale model.

I have the following questions / comments for the authors:

1. It is known that the measured data of static pressure is very sensitive to the shape around the pressure hole on the flow surface. The used pressure taps in the experiments are 5mm thickness frustum. Did the authors confirm the effect of the shape and thickness of this tap on the measured data of static pressure by calibration test, for example, using wind tunnel?
2. I am very interested in the differences of pressure distributions between wind tunnel and on-water which are shown in Figure 9. As mentioned by the authors in Section 3.4, the *Cp*s measured in full scale show only one suction peak near the leading edge. Conversely, the *Cp*s measured in the wind tunnel show two suction peaks and this is correlated with the reattachment of the laminar separation bubble. Therefore, the differences between the full scale and wind tunnel pressure distributions could be the result of the absence of the laminar separation bubble during the full scale experiment.

The authors also describe that the formation of a leading edge separation bubble would be more likely in the wind tunnel with its lower turbulence intensity, and also at the lower Reynolds number. However, they consider that it is more likely that the differences in pressure distributions are the result of different sail trims rather than Reynolds number effects or to different turbulence characteristics of the flows.

However, I would like to think these differences in pressure distributions are caused mainly by the Reynolds number effects.

Wind Tunnel tests using model sails are commonly performed at the Reynolds number region of around $2x10^5$ to $5x10^5$. This region is referred to as the critical Reynolds number range, where the boundary layer flow turns from laminar to turbulent, causing the drag and lift coefficients to change drastically. Hoerner [1] shows experimental results of wing sections in this region and indicates that the maximum lift coefficient varies as a function of the Reynolds number, camber ratio and nose-radius ratio, and also can be very sensitive to the test conditions.

A spinnaker has a large camber and a sharp leading edge which works at a high entrance angle. As mentioned by the authors, this causes the laminar-type separation at the suction side of the leading edge and forms the laminar separation bubble at the low Reynolds number region.

From my experience of wind tunnel tests using downwind sails at $Re=2.9x10^5$, I sometimes experienced that the slight shape change of a spinnaker by sheet trimming caused serious deviation on measured aerodynamic forces. This deviation of forces sometimes occurred more than several seconds later after the sheet trimming, although the shape of the sails scarcely varied during this deviation of the forces. Therefore, I thought this unstable deviation of the forces was caused by the behavior of the laminar separation bubble, which can easily spread over the surface of the suction side at the low Reynolds number.

On the other hand, for the full scale boat, the sails work in the Reynolds number of almost greater than $1x10^6$. In this region, although the effect of critical Reynolds number still remains, the effect on the measured data may be less than the case of wind tunnel tests.

In this point of view, I think this paper shows an epoch making result which indicates the absence of the laminar separation bubble at the leading edge during the full scale experiment. I hope that the full scale measurements of the pressure distributions on the full scale downwind sails will be continued by the authors in order to clarify the main reason of the differences of pressure distributions.

I would like to hear the opinion of the authors about this point.

ADDITIONAL REFERENCES

Hoerner, S. F., and Borst, H. V., 'Fluid-dynamic Lift,' Hoerner Fluid Dynamics, p.4-12, 1975.

Robert Ranzenbach, Member

The authors provide the sail analysis/testing/design community a good service by comprehensively comparing the utility of numerical modeling, wind tunnel testing, and on-water full-scale measurements to define the aerodynamics of offwind sails.

As noted in the paper, much of the experimental evidence collected to date has been focused on global aerodynamic forces and this additional data will prove invaluable to our understanding of the underlying physics of asymmetric spinnakers and to anyone interested in validating their CFD predictions of this complex, three-dimensional, separated flow.

The authors are to be congratulated on their meticulous effort to obtain pressure measurement data on a flexible membrane like an asymmetric spinnaker. The authors identify the challenges of establishing reference conditions and further work is clearly warranted in this area. Given the large variation in the direction of the oncoming flow, it may be prudent to consider higher order multi-hole probes to reduce/eliminate uncertainty regarding the dynamic pressure of the oncoming flow.

The hypothesis posited on page 9 by the authors regarding the impact to the pressure results from the relative tightness of trim during full-scale measurements compared to that of the wind tunnel ("A tighter trim is thought to have been used in the full-scale measurements as a result of having to trim in the unsteady wind conditions. Conversely, the stationary wind conditions and fixed yacht model attitude in the wind tunnel allowed a more eased trim to be used."), might be easily tested by returning to the wind tunnel and repeating the test conditions in a slightly over-trimmed state and then comparing these new pressure measurement results.

I note with interest the assertion that the results in "Figure 9 shows good agreement and similar trends between the Cps measured in full scale and in the wind tunnel" when later in the paper is it noted that "the wind tunnel tests were carried out in uniform untwisted flow" whereas the full-scale measurements were carried out in necessarily twisted flow. Given that correctly modeling environmental and boundary conditions is a central tenet of being able to compare these types of results between two testing modalities, I look forward to learning more about how twisted flow changes the pressure distribution on offwind sails and whether this influence helps close the gap between model-scale wind tunnel measurements and on-water full-scale measurements.

Tom Schnackenberg, Visitor

I enjoyed reading this paper very much, and was impressed with the thought that had gone into all the interpretations of data. The "delta-wing" pressure distribution at the head was particularly interesting.

One thing that left me feeling vaguely dissatisfied was the discussion of pressure measurements. The static atmospheric pressure decreases by about 12 Pa per metre with increasing elevation, which is significant, and I am wondering the effect of this on pressure measurements at different heights. I believe it would enhance the paper if this was covered in the discussion.

Reading paragraphs 2.1 and 2.3, I deduce that the pressure sensors were on the port side of the sail, and that the pitot-static probes were always on the windward side of the yacht. If I am right then this fact could perhaps be made clearer. I found the language a little obtuse here.

I was surprised by the CFD result quoted in 2.3 that the dynamic pressure was higher at the probes than is it in the far field. If the probes are to the windward side of the sail set, one might expect lower velocities and hence lower dynamic pressures than in the far field.

These are just quibbles really, and I could easily be wrong. Overall, I think it is a very interesting paper.

Authors' Response

The authors are very grateful for the several interesting comments and suggestions received from their colleagues, and are sorry if it is not possible to address each of the raised points within the space allowed.

Reynolds Number

One of the key open questions is whether the observed differences on the pressure distributions measured in full-scale and model-scale are due to the different Reynolds numbers. In fact, as very well pointed out by Emeritus Professor Masuyama, sails are tested in the wind tunnel at Reynolds number of the order of 10^5, while in full scale sails operate at Reynolds number of the order of 10^6. Figure AR-1 (from Hoerner and Borst, 1985, Sec. 4-11) shows the maximum lift coefficient (C_{LX}) versus the chord Reynolds number (R_C) for different foils with sharp leading edges. At R_C lower than 10^6, such as in the wind tunnel, the maximum lift is independent from R_C, while for R_C greater than 10^6, such as in full-scale, the maximum lift increases with R_C.

The improved performances at high R_C are due to the laminar-to-turbulent transition in the laminar separation bubble that leads to a shorter bubble and thus to higher lift. In fact, Figure AR-2 (from Hoerner and Borst, 1985, Sec. 4-3) shows that the laminar separation bubble is correlated with a pressure plateau on the sail surface and, therefore, the leading edge suction is lower with the bubble than without the bubble. Increasing the angle of attack, the laminar separation bubble length increases and stall occurs when its length is longer than the chord. The higher the Reynolds number, the shorter the bubble and the higher the stall angle of attack. This behavior is typical of foils with sharp leading edge and very small camber, such as double wedged profiles (Fig. AR-2) and flat plates (e.g. Crompton and Barrett, 2000).

The authors believe that sails behave differently from the profiles presented by Hoerner and Borst and therefore the sensitivity from the Reynolds number is different. Firstly, the laminar separation bubble on sails is normally confined within the first few percentages of the chord. Secondly, near the leading edge, sails present a very high suction peak instead of a pressure plateau. Finally, the stall is due to trailing edge separation and not to leading edge separation.

The two typical suction peaks on the leeward side of sails are due to inviscid effects and exist even without laminar separation bubble. Using the linearity of the Laplace equation, it is possible to split the pressure distribution on a curved plate with the contribution due to the angle of incidence and the contribution due to its curvature (Fig. AR-3). The sum of these two pressure distributions results in two suction peaks. The effect of the viscosity is to damp the infinitely low suction at the leading edge and, if separation occurs, to form a pressure plateau near the trailing edge (dotted lines in Fig. AR-3).

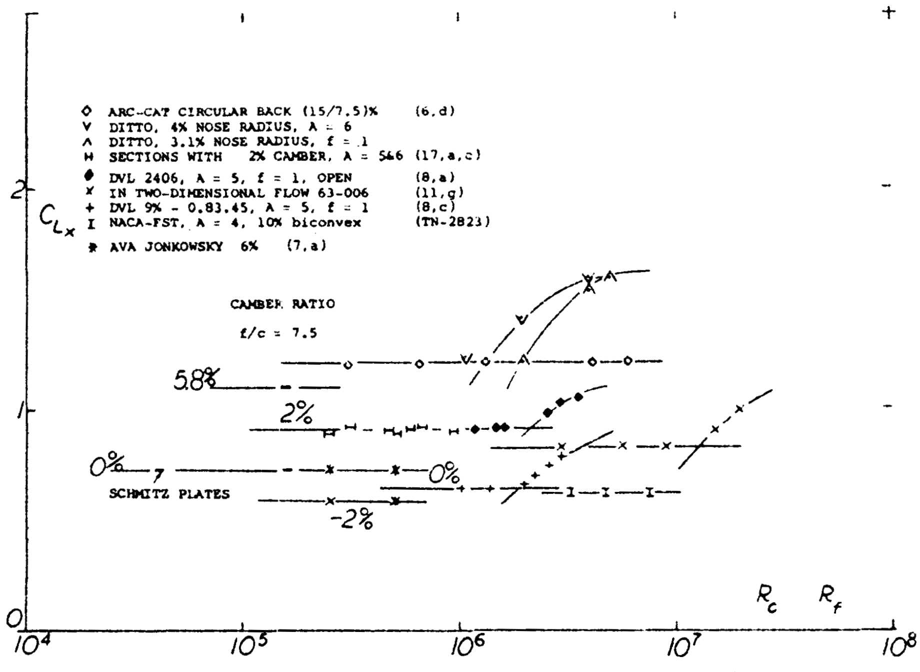

Figure AR-1: Maximum lift of rectangular foils versus the Reynolds number for different sections with sharp leading edges (Hoerner and Borst, 1985)

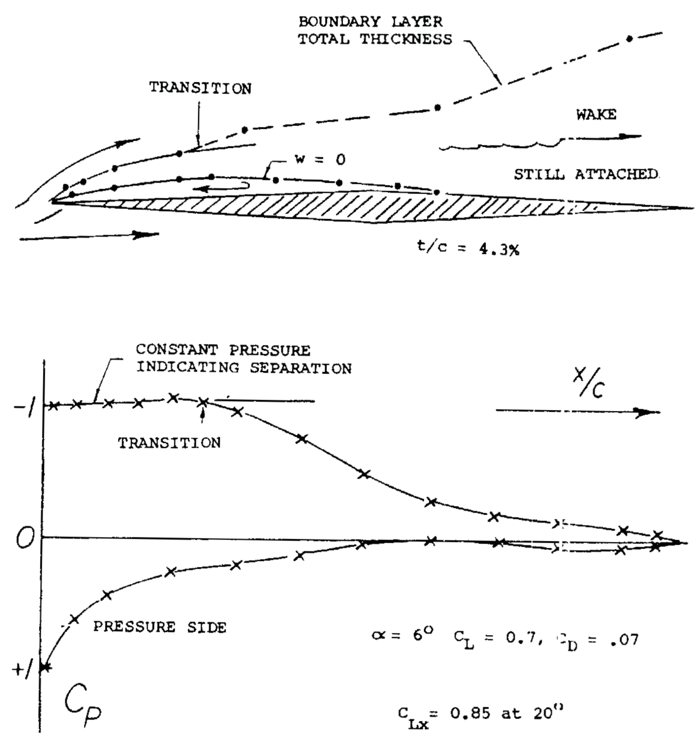

Figure AR-2: Break down of the pressure distribution with potential flow theory

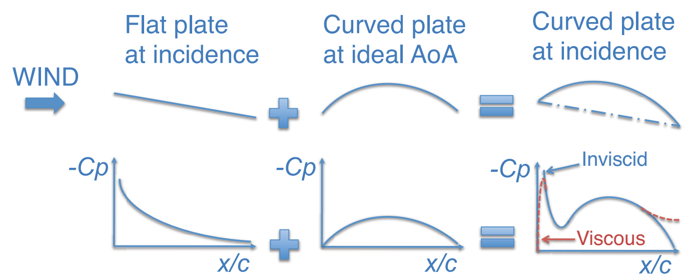

Figure AR-3: Break down of the pressure distribution

Numerical simulations performed with a viscous-flow solver (Viola et al., 2013) computed pressure distributions in very good agreement with wind-tunnel measurements (Viola et al., 2011) and revealed that the laminar separation bubble reattached just upstream of the maximum pressure recovery. Simulations performed with an inviscid-flow solver (Viola et al., 2011), which did not take into account the laminar separation bubble, computed pressure distributions still in good agreement with wind-tunnel measurements (Fig. AR-4), though predicted a higher and more upstream pressure recovery than the experiment. As expected, the highly viscous flow in the laminar separation bubble tends to smooth the pressure distribution, which is in agreement with the smoothed pressure gradients reported by Hoerner and Borst, 1985.

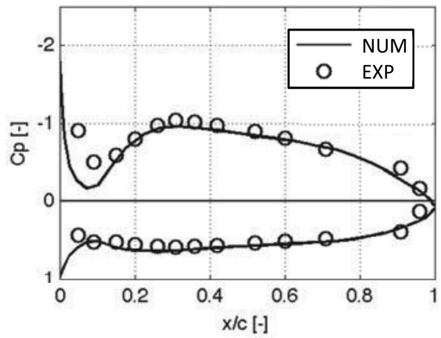

Figure AR-4: Pressure distribution computed with potential flow method and measured experimentally (Edited from Viola et al., 2011)

The effect of the viscosity presented in Figs. AR-3 and AR-4 allows foreseeing that, at high Reynolds numbers, both the leading edge suction peak and the pressure recovery may be sharper than at low Reynolds numbers. Conversely, in the present paper, the pressure distributions measured at low-Reynolds numbers in the wind tunnel are sharper than those measured at high Reynolds numbers in full scale. For this reason, the authors believe that the observed differences are most likely due to a tighter sail trim.

This conclusion is further supported by full-scale tests on upwind sails (Viola and Flay, 2010a), where pressure distributions were measured for different sail trims. Figure AR-5 (from Viola and Flay, 2010a) shows the pressure distributions on three sections of the genoa for five trims, where 0 stands for the looser trim and +4 stands for the tighter trim. The differences between the pressure distributions +1 and +2 are similar to those between model scale and full scale on the present paper.

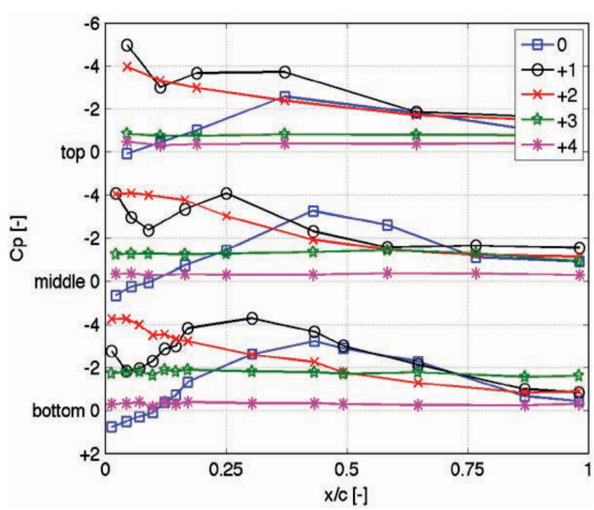

Figure AR-5: Pressure distributions measured in full-scale on three sections of a genoa in upwind conditions (from Viola and Flay, 2010a).

It is interesting to note that sails stall because of trailing edge separation, which, indeed, is highly dependent on the Reynolds number. For instance, the maximum lift of NACA sections such as 65_3-618 may increase by more than 20% when the Reynolds number increases from 3 million to 9 million (Abbott and Von Doenhoff, 1959). Therefore, it is expected that the Reynolds number may affect more significantly the pressure distribution near the trailing edge than the one near the leading edge. In particular, the higher the Reynolds number, the higher the second suction peak could be.

Twisted Flow

As highlighted by Dr. Ranzenbach, the differences between full scale and model scale may also be partially due to the twisted flow, which was not modelled in model scale. In particular, in full scale, AWA = 80 deg at the top of the mast and thus AWA at the foot of the sail is approximately 75 deg. Therefore, in model scale, where AWA = 70 deg, the AWA was lower than in full scale by 5 to 10 deg. However, a uniform shift of AWA from 70 deg to 80 deg would be negligible for the pressure distributions. In fact, if the sail was trimmed at the optimum trim in both conditions, the position of the sail with respect to the wind would be almost identical and so the pressure distributions. On the other hand, even if the sail was twisted accordingly to the wind twist, the relative different AWA from the lowest to the highest section may lead to different pressure distributions due to different span-wise wind velocity components. This effect cannot be quantified with the available data, however Viola and Flay (2010b) performed model-scale pressure measurements with and without twist, and they observed smaller differences than those in the present paper for a much higher twist angle (approx. 25 deg). Therefore, it seems that the different twist between full scale and model scale cannot explain the observed different pressure distributions.

Flying Shape Detection

Flying shapes were measured taking several photographs of the sails and processing the photographs with photogrammetric techniques. In particular, pressures were measured for 90 s and in this time interval a fast powerboat was able to sail around *Aurelie* taking several photographs of the sails. Unfortunately this procedure led to poor measurement accuracy, which was insufficient to identify differences between model-scale and full-scale shapes.

Maximum Drive-force Trim

Since neither force measurements nor accurate flying shape measurements are available, it is not possible to know if the *max-eased* trim allowed higher drive force that the *eased* trim. However, considering that most of the drive force is due to the suction in the region near the leading edge due to its favourable orientation, the *eased* trim is likely to generate more drive force than the *max-eased* trim on the highest sections and vice versa on the lowest sections.

Pressure Taps

The pressure taps were embedded between two layers of sailcloth and thus the sail surface was smooth and it was assumed that the taps had no effects on the local flow field. However, the double layer of sailcloth, the taps and the tubes increased the stiffness of the sails in a non-uniform manner. As correctly pointed out by Peter Heppel, this effect may be significant and should be further investigated.

Only the layer of sailcloth on the port side had a hole that allowed the pressures to be transmitted to the pressure taps. Therefore the pressures were always measured on the port side. Conversely, the pole supporting the Pitot-static probes was always on the windward side. Therefore, leeward pressures were measured sailing on a starboard tack with the pole on the starboard side, while windward pressures were measured sailing on a port tack with the pole on the port side.

Elevation of the Pressure Tap

Dr. Schnackenberg correctly highlighted that the measured pressures are, indeed, net of the hydrostatic pressure. In fact, the hydrostatic contribution of the pressure varied inside the pressure tube from the tap to the transducer. The measured pressure difference is the difference between the static pressures at the two sides of the transducers, and therefore it is the difference between the pressure inside the cabin and the pressure on the sail surface net of the hydrostatic pressure.

Future Work

Further research on full-scale pressures may allow addressing some of the several questions left open from this discussion. Very importantly, flying shapes must be detected with higher accuracy in order to allow a comparison with numerical and physical models. Also, long pressure tubes must be avoided in order to allow measuring high frequency pressure signals. In fact, as suggested by Peter Heppel, spectral analysis would allow the contribution of the turbulent free stream and of the local boundary layer to be identified. Also, the analysis of the different pressure taps along a streamline will allow new insights on the location of the laminar-to-turbulent transition and on the dynamics of the separation and reattachment points.

ADDITIONAL REFERENCES

ABBOTT, I.H., Von Doenhoff, A.E., Theory of Wing Sections, Including a Summary of Airfoil Data, Dover Publications, Inc., New York, 1959.

CROMPTON, M.J., Barret, R.V., Investigation of the separation bubble formed behind the sharp leading edge of a flat plate at incidence, *Proc. Inst. Mech. Eng., Part G: J. Aerospace Eng.,* 2000; 214 (3), 157–176.

HOERNER, S.F., Borst, H.V., Fluid-Dynamic Lift: Information on Lift and Its Derivatives in Air and Water, *Hoerner Fluid Dynamics*, Bakersfield, CA, 1985.

VIOLA I.M., Flay R.G.J., Full-scale Pressure Measurements on a Sparkman & Stephens 24-foot Sailing Yacht, *Journal of Wind Engineering and Industrial Aerodynamics,* 2010a; 98, 800-807.

VIOLA I.M., Flay R.G.J., Pressure Distribution on Modern Asymmetric Spinnakers, *International Journal of Small Craft Technology, Trans. RINA,* 2010; 152 (B1) 41-50.

VIOLA I.M., Flay R.G.J., Sail Aerodynamics: Understanding Pressure Distributions on Upwind Sails, *Experimental Thermal and Fluid Science*, Nov 2011; 35 (8), 1497-1504.

VIOLA I.M., Pilate J., Flay R.G.J., Upwind Sail Aerodynamics: a Pressure Distribution Database for the Validation of Numerical Codes, *International Journal of Small Craft Technology, Trans. RINA,* 2011; 153 (B1), 47-58.

VIOLA I.M., Bot P., Riotte M., Upwind Sail Aerodynamics: a RANS Numerical Investigation Validated with Wind Tunnel Pressure Measurements, *International Journal of Heat and Fluid Flow*, in press, expected 2013. DOI: 10.1016/j.ijheatfluidflow.2012.10.004.